Effect of inelastic coupling on 0^+ analog transitions†

V. A. Madsen,* V. R. Brown, S. M. Grimes, C. H. Poppe,‡
J. D. Anderson, J. C. Davis, and C. Wong
Lawrence Livermore Laboratory, Livermore, California 94550
(Received 21 August 1975; revised manuscript received 28 October 1975)

A comparison is made between experimental cross sections for the (p, n) reaction to the ground-state analogs of the isotopes ^{92}Mo, ^{98}Mo, ^{100}Mo, and coupled-channel calculations including coupling to the 2^+ and 3^- inelastic states and their analogs. When the coupling is included, very good fits are obtained for the (p, n) 0^+ analog differential cross section using uniform optical parameters for all three isotopes. Experimentally observed variations of about 50% in $\sigma/(N-Z)$, which in distorted-wave Born approximation changes by only 10%, are explained by the coupling. A crude third-order distorted-wave Born approximation model is developed which shows that the three-step amplitudes $0^+ \rightarrow 2^+ \rightarrow 2^+$ analog $\rightarrow 0^+$ analog, $0^+ \rightarrow 2^+ \rightarrow 0^+ \rightarrow 0^+$ analog, and $0^+ \rightarrow 0^+$ analog $\rightarrow 2^+$ analog $\rightarrow 0^+$ analog are all in phase and are destructive to the dominant one-step $0^+ \rightarrow 0^+$ analog amplitude.

[NUCLEAR REACTIONS ^{92}Mo, ^{98}Mo, ^{100}Mo(p,n); measured 2^+, 3^- analog cross sections at 18, 22, 26 MeV; 0^+, 2^+, and 3^- analog $\sigma(\theta)$ at 16 and 26 MeV calculated including coupling to inelastic channels.]

I. INTRODUCTION

In a recent study[1,2] of the (p,n) reaction on the isotopes of molybdenum, the analog cross section shows an energy dependence and departs considerably from the Lane-model prediction of near proportionality to $(N-Z)$. Coupled-channel calculations[2] indicate that the $(N-Z)$ effect can be explained by coupling to the 2^+ first excited state and its analog. By now it is well known[3] that the excitation of analogs of strong collective states proceeds primarily by two two-step mechanisms as shown in Fig. 1(a), the one-step process being negligibly small.[4] In Sec. II of this paper it is shown that the three three-step processes in Fig. 1(b) have amplitudes that are nearly in phase with each other and add destructively to the dominant one-step mechanism for the 0^+ analog transition. Therefore, when the 2^+ states are coupled, the cross section for the 0^+ analog state decreases by an amount that is roughly proportional to the inelastic (p,p') 2^+ cross section. In the case of the molybdenum isotopes, the 2^+ inelastic cross section increases by a factor of about 5 between ^{92}Mo and ^{100}Mo. The excited 2^+ analog (p,n) transition should then be much stronger in ^{100}Mo than in ^{92}Mo. The 3^- inelastic states are also excited strongly in Mo(p,p'), and there is substantial variation from ^{92}Mo to ^{100}Mo. It is shown in this paper that it is important for consistency from isotope to isotope to include in the calculation of 0^+ analog cross sections the coupling of the 2^+ and, to a lesser extent, the 3^- states.

In Sec. III the measured (p,n) cross sections at 18, 22, and 26 MeV leading to the 2^+ and 3^- analog states are presented for ^{92}Mo, ^{98}Mo, and ^{100}Mo along with calculations for 16 and 26 MeV protons in which the 0^+, 2^+, and 3^- states and their analogs are simultaneously coupled.[5] The strength parameters $\beta_{pp'}$ are taken from the literature and the Lane potential V_1 is scaled to fit the data but is constrained to be the same for all three isotopes at a given energy. Comparison with the measured 2^+ and 3^- analog (p,n) cross sections provides a consistency test for the calculations. The agreement between theory and experiment for all the analog cross sections in all three isotopes shows that the coupling of the 2^+ state does account for the deviation of $\sigma/(N-Z)$ from near constancy.

II. PHASE OF THE THREE-STEP AMPLITUDES

When strong coupling is used instead of distorted-wave Born approximation (DWBA) for the $0^+ \rightarrow 2^+$ inelastic transition, its cross section is reduced. (To compensate one must reduce the imaginary potential from that given by the optical model, because one of the channels for removal of flux is now included explicitly.) In perturbation theory the reduction in cross section comes in leading order from the third-order process shown in Fig. 2. The third-order amplitude must then be destructive when added to the dominant first-order term. In the case of analog transitions the three steps are made up of one analog and two in-

elastic steps as shown in Fig. 1(b), the two inelastic steps being just of the kind seen in Fig. 2. If all the three-step amplitudes are equal and small compared to the one-step part, we expect that to leading order the fractional reduction will be a factor of 3 greater for the analog than for the inelastic scattering transition when the couplings of Figs. 1 and 2, respectively, are included. Results of an actual coupled-channel calculation, which treats the reaction to all orders, is shown for comparison in Table I.

In an attempt to understand these results we obtain below a crude approximation to the first- and third-order amplitudes in charge-exchange processes,

$$A^{(1)} = \langle \chi_2^{(-)} | V | \chi_1^{(+)} \rangle , \tag{1a}$$

$$A^{(3)} = \langle \chi_2^{(-)} | VG_1 VG_3 V | \chi_1^{(+)} \rangle , \tag{1b}$$

$$A^{(3)'} = \langle \chi_2^{(-)} | VG_4 VG_2 V | \chi_1^{(+)} \rangle , \tag{1c}$$

$$A^{(3)''} = \langle \chi_2^{(-)} | VG_4 VG_3 V | \chi_1^{(+)} \rangle , \tag{1d}$$

where the initial and final state or intermediate Green's function have the appropriate channel label n as in Fig. 1(a). The wave functions and Green's functions are given by

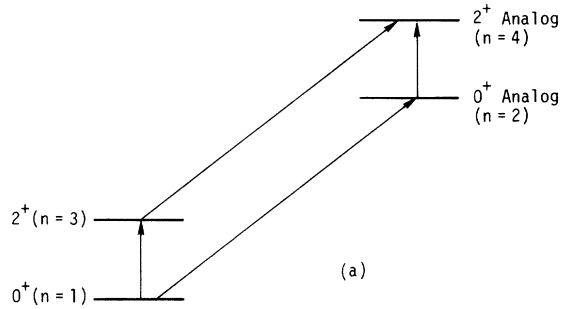

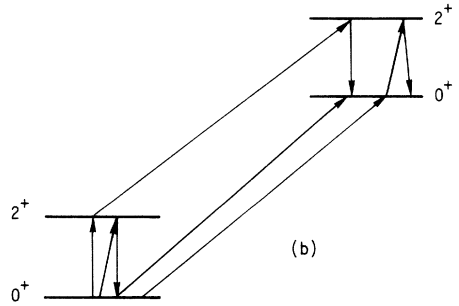

FIG. 1. (a) The primary mechanism for the (p,n) reaction to analogs of excited states is the two-step mechanism shown. The letter n is a channel label. (b) These three-step processes contribute to reduction for the ground-state analog cross section.

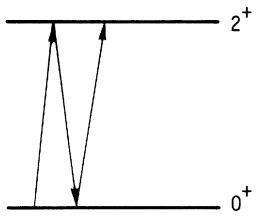

FIG. 2. The three-step transition shown contributes to a reduction in the 2^+ inelastic cross section.

$$\chi_1 = \Phi_1 \chi_1(\vec{r}) = \Phi_1 4\pi \sum_{L\,M} i^L Y_L^{M*}(\hat{k}) Y_L^M(\hat{r}) R_L(kr) , \tag{2a}$$

$$G_1 = |\Phi_1\rangle g_1 \langle \Phi_1| , \tag{2b}$$

where Φ_1 is the wave function for the target in channel 1, and the Green's function is given by

$$g_1(\vec{r},\vec{r}') = a_1 \sum_{l_1 m_1} Y_{l_1}^{m_1 *}(\hat{r}) Y_{l_1}^{m_1}(\hat{r}') R_{l_1}(r_<) R_{l_1}^+(r_>) , \tag{3a}$$

$$a_1 = \frac{2m}{\hbar^2}\frac{k_1}{i} \tag{3b}$$

In Eq. (3a) R_{l_1} is the regular solution and $R_{l_1}^+$ is the outgoing solution of the optical-model radial Schrödinger equation with the asymptotic boundary conditions,

$$R_l \to \tfrac{1}{2}\left[e^{2i\delta_l} H_l^{(1)}(kr) + H_l^{(1)*}(kr) \right] , \tag{4}$$

$$R_l^+ \to H_l^{(1)}(kr) \to (kr)^{-1} \exp i[kr - (l+1)\pi/2 - \eta \ln(2kr) + \sigma_l] .$$

Evaluating the nuclear matrix elements leaves the result

$$A^{(3)} = \sum_\mu \int \chi_2^{(-)*}(\vec{r}) V_{21}(\vec{r}) g_1(\vec{r},\vec{r}') V_{13}^\mu(\vec{r}') g_3(\vec{r}',\vec{r}'') \times V_{31}^\mu(\vec{r}'') \chi_1^{(+)}(\vec{r}'') d^3r d^3r' d^3r'' , \tag{5}$$

and similarly for the other amplitudes. As the aim of this development is to try to get a simple qualitative picture of the behavior of the three-step amplitude, we make the simplifying assump-

TABLE I. Comparison of DWBA and coupled-channel (C. C.) runs for the 16 MeV ^{100}Mo (p,p') and (p,n) 0^+ transition. The 0^+ ground state, the 2^+ and 3^- excited states, and their analogs are coupled.

Case	$\sigma(p,p')$ 2^+ (mb)	$\sigma(p,n)$ 0^+ (mb)
DWBA	41.4	5.15
C. C.	30.6	2.21

tion that all the interactions have surface δ functions as their radial form:

$$V_{21}(r) = X_1 \delta(r-R), \tag{6a}$$

$$V^{\mu}_{31}(r) = Y^{\mu}_{2}{}^{*}(\hat{r}) X_0 \delta(r-R), \tag{6b}$$

$$V^{\mu}_{13}(r) = Y^{\mu}_{2}(\hat{r}) X_0 \delta(r-R). \tag{6c}$$

The constants X_1 and X_0 are complex numbers proportional to the Lane interaction and the optical-potential strengths, respectively, and both also contain the nuclear matrix elements. Using the expansions Eqs. (2) and (3) and Eq. (6) one can readily evaluate the three-step amplitudes. The first-order and third-order amplitudes are

$$A^{(1)} = \sum_{LM} A^{(1)}_{LM} = (4\pi)^2 X_1 \sum_{LM} Y^{M}_{L}(\hat{k}_2) Y^{M}_{L}{}^{*}(\hat{k}_1) R_L(k_2 R) R_L(k_1 R) R^2, \tag{7a}$$

$$A^{(3)} = X_0{}^2 R^4 \sum_{LM} A^{(1)}_{LM} \hat{L}^{-2} \sum_{l} \langle l || Y_2 || L \rangle^2 \begin{cases} a_1 a_3 R_L(k_1 R) R^{+}_{L}(k_1 R) R_l(k_3 R) R^{+}_{l}(k_3 R) \\ a_4 a_2 R_l(k_4 R) R^{+}_{l}(k_4 R) R_L(k_2 R) R^{+}_{L}(k_2 R) \\ a_4 a_3 R_l(k_4 R) R^{+}_{l}(k_4 R) R_l(k_3 R) R^{+}_{l}(k_3 R), \end{cases} \tag{7b}$$

where the three lines in Eq. 7(b) refer to the three different amplitudes of Fig. 1(b). To proceed further we need to put in some information about the various radial wave functions. Since we have evaluated them all at the nuclear surface, we take as a rough approximation just the asymptotic forms. The radial Green's function of equal argument R is

$$g^{+}_{l}(R,R) = \frac{2mk}{\hbar^2 i} R_l(kR) R^{+}_{l}(kR) \rightarrow \frac{2m}{\hbar^2} \frac{k}{i} \tfrac{1}{2} [e^{2i\delta_l} H^{(1)}_{l}(kR) + H^{(1)}_{l}{}^{*}(kR)] H^{(1)}_{l}(kR)$$

$$= \frac{m}{\hbar^2} \frac{k}{i} \{ [e^{i\delta_l} H^{(1)}_{l}(kR)]^2 + |H^{(1)}_{l}(kR)|^2 \}. \tag{8}$$

The first term we drop on the grounds that, because of the complex plase shift, it is small compared to the second term. In addition, if instead of using a δ function in the surface we had integrated over 2 to 4 fm of nuclear surface, the oscillatory nature of $[H^{(1)}_{l}(kr)]^2$ would cause phase cancellation, further reducing its contribution. We recognize this as a crude approximation designed to show the main effects of the three-step process. Numerical calculations are expected to show substantial deviations from the result we get using Eq. (8). From Eq. (7b) and Eq. (8) it follows that the three third-order amplitudes are

$$A^{(3)} \approx -\left(\frac{m}{\hbar^2}\right)^2 X_0{}^2 R^4 \sum_{LM} A^{(1)}_{LM} \hat{L}^{-2} \sum_{l} \langle l || Y_2 || L \rangle^2 \begin{cases} k_1 k_3 |H^{(1)}_{L}(k_1 R)|^2 |H^{(1)}_{l}(k_3 R)|^2 \\ k_4 k_2 |H^{(1)}_{l}(k_4 R)|^2 |H^{(1)}_{L}(k_2 R)|^2 \\ k_4 k_3 |H^{(1)}_{l}(k_4 R)|^2 |H^{(1)}_{l}(k_3 R)|^2. \end{cases} \tag{9}$$

The three three-step amplitudes are exactly in phase and are nearly equal. If X_0 were purely real, each $A^{(3)}$ term of Eq. (9) would be exactly out of phase with the $A^{(1)}$ terms and, because of the $X_0{}^2$, proportional to the inelastic cross section. In fact, $X_0{}^2 \propto (-|V_0| - i|W_0|)^2 = (V_0{}^2 - W_0{}^2) + 2i|V_0||W_0|$. For a typical value $W_0 = \frac{1}{3} V_0$ the phase of this complex constant is 146°, and its cosine is −0.829, so it is still very nearly completely destructive. Figure 3 shows the result of an amplitude calculation using $W_0 = 0$ done with the Oregon-State coupled-channel code.[6] Plotted are the phase angles ϕ_1 and ϕ_3 of the amplitudes as a function of scattering angle for $A^{(1)}$ and $A^{(3)}$. Also shown is the phase difference $\phi_3 - \phi_1$ and the constant 180° prediction of Eq. (9) with X_0 real. The hatched band shows the region in which $\cos(\phi_3 - 180°)$ differs from 1 by less than 20%. The agreement is satisfactory, and the technique gives us a way of understanding the relative phases of multistep processes.

III. EXPERIMENTAL CROSS SECTIONS AND COMPARISON TO RESULTS OF COUPLED-CHANNEL CALCULATIONS

The (p,n) ground-state analog cross sections of the Mo isotopes have been reported previously[1,2] between 16 and 26 MeV. Because of the smaller yields, measurement of the 2^+ and 3^- (p,n) excited analog cross sections required longer runs to obtain adequate counting statistics. A time-of-flight spectrum for ^{100}Mo at $E_p = 26$ MeV and $\theta_{lab} = 61°$ is shown in Fig. 4. The graphical method[7] for extrac-

tion of excited-analog-state cross sections was used. In addition to the graphical method, the 2^+ and 3^- cross sections were extracted using a computer code which simultaneously fitted excited and ground-state analog peaks in the neutron time-of-flight spectra. In all cases there was good agreement between the cross sections obtained graphically and those obtained using the computer-generated fits.

Coupled-channel calculations have been performed with the Oregon-State coupled-channel code[6] for ^{92,98,100}Mo(p,n). These three isotopes, having empirical deformation parameters[8] $\beta_2 = 0.105$, 0.168, 0.226, respectively, cover the range from a very weak to intermediate to a very strong 2^+ excitation. Thus we expect the 2^+ coupling effect to be smallest in ^{92}Mo and largest in ^{100}Mo. In addition to the strong 2^+ excitations these isotopes have fairly strong 3^- excitations with deformation parameters[8] $\beta_3 = 0.174$, 0.195, 0.210. We have therefore included both the coupling of the 2^+ and 3^- states[5] in our calculation. Our procedure for obtaining optical parameters is the following: There exist[8] both 2^+ and 3^- (p,p') data for Mo at 16 MeV from which β_2 and β_3 have been extracted. Starting with the Becchetti-Greenlees (BG) global proton optical parameters,[9] we decreased the magnitude of all imaginary optical potentials by 12% to account for the explicit inclusion of the coupling. Finer adjustment on the individual inelastic cross sections was then done for ^{92}Mo by lowering β_2 by 12% from that of Ref. 8 to 0.092. These parameters gave good fits to all the (p,p')

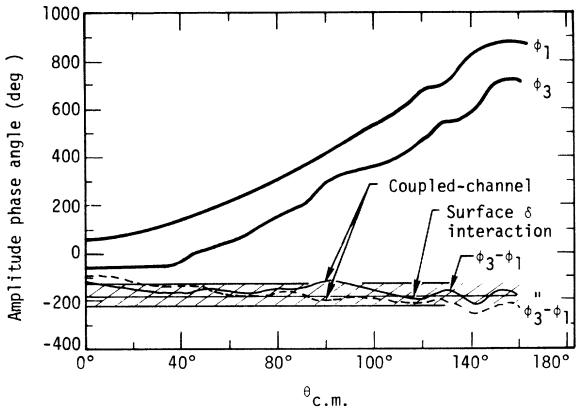

FIG. 3. A comparison of the complex phase angles ϕ_1 and ϕ_3 of the one- and three-step amplitudes. The phase angles ϕ_3 and ϕ_3'' are for two of the three three-step processes which contribute destructive interference to the one-step amplitude. The cosine of any difference angle in the hatched region is between -0.8 and -1.0. The calculation is done for the ^{100}Mo(p,n) 0^+ analog at $E_p = 26$ MeV.

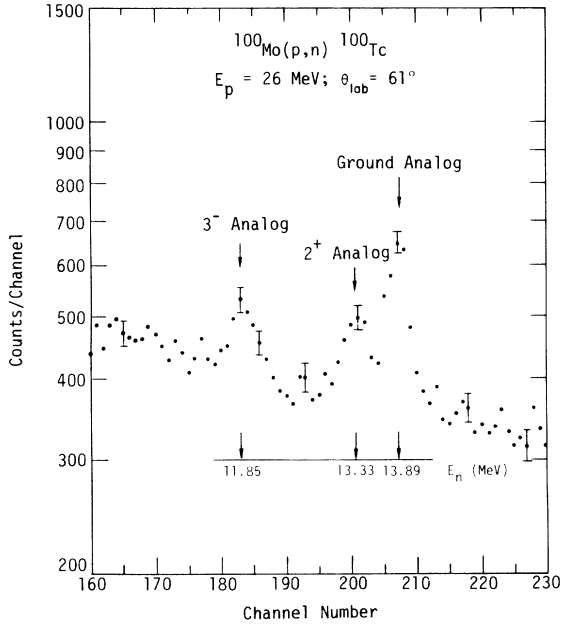

FIG. 4. Time-of-flight spectrum for ^{100}Mo(p,n) at $E_p = 26$ MeV and $\theta_{lab} = 61°$ with increasing flight time towards the left. The flight path was 10.8 m; the detector was an 11.4 cm diam by 5.1 cm long NE213 scintillator; the bombardment charge was 3300 μ C; the time calibration was 0.71 ns/channel.

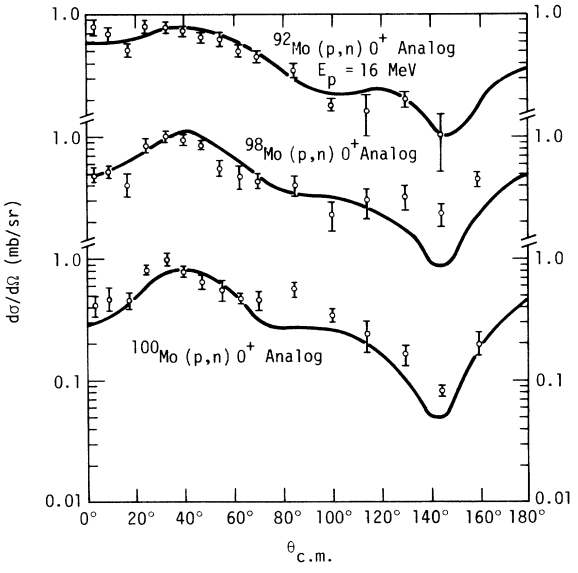

FIG. 5. Coupled-channel calculations, including 2^+ and 3^- inelastic states, of the 16 MeV Mo(p,n) transition to the 0^+ analog states. Global optical parameters of Becchetti and Greenlees (Ref. 9) were used except for uniform adjustments of all imaginary potentials and Lane isospin potentials as described in the text.

TABLE II. Comparison of Lane potentials V_1 and W_1 used with coupling (in coupled-channel calculations including 2^+ and 3^- coupling as explained in the text) and without coupling (from Ref. 2 based on V_1, W_1 searches for individual isotopes not including 2^+ and 3^- inelastic coupling). Energies and potentials are in MeV.

Case	Energy	Potential	^{92}Mo	^{98}Mo	^{100}Mo
Without	16	V_1	125.5	97.8	92.8
		W_1	12.2	27.0	23.9
With		V_1	115.2	All isotopes	
		W_1	50.7		
Without	26	V_1	77.9	66.7	64.9
		W_1	39.0	35.4	39.4
With		V_1	86.4	All isotopes	
		W_1	38.0		

data in the coupled-channel calculations. The Lane potentials V_1 and W_1 from Ref. 9 were then adjusted uniformly for all isotopes at each energy to get the best over-all agreement with the experimental analog cross sections. The value needed at the 16 MeV proton energy is 1.2 times those of Ref. 9. The calculated 0^+ analog cross sections are shown in Fig. 5. The fits are excellent except that in ^{100}Mo(p,n) the calculated cross section is somewhat low at the middle angles. It is interesting to note that the coupled-channel calculations using global parameters[9] adjusted uniformly as described above give nearly the same angular distributions as those obtained[2] by searches on the isospin strength for individual isotopes but with only the coupling to the 0^+ analog state included. A comparison of isospin strength parameters used in Ref. 2 and in the coupled-channel calculations is given in Table II. (These fits are much better than those obtained[2] using BG parameters with a search only on the neutron optical potential.)

The same 12% decrease of the imaginary potential was then used for the calculation at 26 MeV. The Lane potentials V_1 and W_1 were adjusted to 0.9 times those of BG, again to fit the (p,n) 0^+ analog data. The comparisons of the calculated cross sections with experiment are shown in Figs. 6–8. The excited-analog-state (p,n) cross sections provide a consistency check on our procedure, since they are sensitive to adjustments made in W, V_1, W_1, and β. The comparisons show that there are no gross errors in our procedure. There appears to be a systematic trend such that the calculated 2^+ analog cross sections are too low for ^{92}Mo and too high for ^{100}Mo. It is possible that this discrepancy is a result of leaving out other possible inelastic couplings, such as to two phonon states,

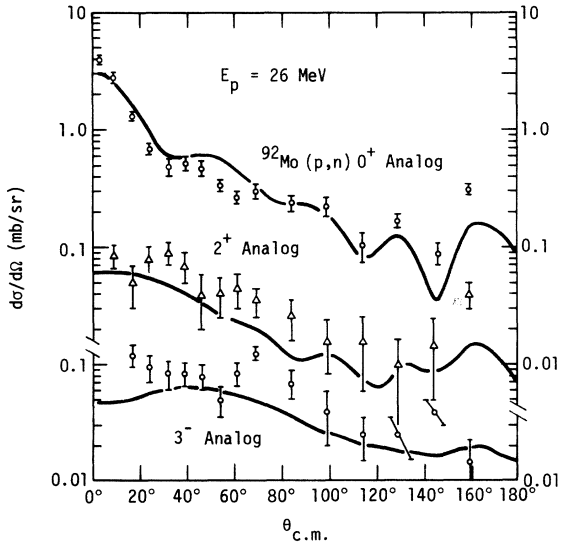

FIG. 6. Coupled-channel calculations including 2^+ and 3^- inelastic states of the 26 MeV ^{92}Mo(p,n) transition to the 0^+, 2^+, and 3^- analog states with global potentials adjusted as in Fig. 5.

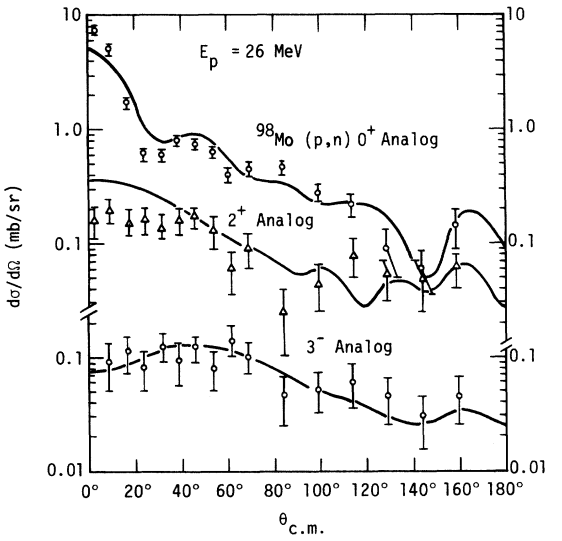

FIG. 7. Same as Fig. 6 but for ^{98}Mo.

which would have the greatest reduction effect in ^{100}Mo. The 3^- analog states in ^{98}Mo and ^{100}Mo are well fitted by the coupled-channel calculations, but the theoretical curve both is low and fails to reproduce the structure of the experimental points in ^{92}Mo.

Figure 9 shows the reduced total 0^+ analog cross section ($\sigma/(N-Z)$) for the three isotopes plotted as a function of the square of the deformation parameter β_2. This quantity is expected[1,2] to change by only about 10% on the basis of first-order direct-reaction theory. It is clear that the calculated inelastic-coupling effect is large and that it explains the trend of the data. The downward adjustment of β_2 suggested above by the comparison of the calculated 2^+ analog cross section in ^{100}Mo with data would move the 0^+ analog to a lower β^2 point on Fig. 9, thereby improving slightly the agreement with experiment.

For completeness analog differential cross sections for the 2^+ states at 18 MeV and 2^+ and 3^- states at 22 MeV are given in Tables III and IV. The total 2^+ analog cross sections are presented in Table V. The cross sections seem to exhibit an energy dependence similar to that of the 0^+ analog.[2] The data are insufficient to establish any energy dependence for the 3^- analog transitions.

IV. SUMMARY AND DISCUSSION

The surprisingly large variation (50%) of the reduced 0^+ analog cross section $\sigma/(N-Z)$ in the (p,n) reaction in the even Mo isotopes is well accounted for by the coupling to the inelastic excited 2^+ and 3^- states and their analogs. The cross section is reduced from the DWBA result primarily by destructive interference with three three-step processes, each of which includes an inelastic excitation and deexcitation and one charge-exchange transition. The destructive phase, predicted by a crude third-order DWBA formula, is verified by calculations of the three-step ampli-

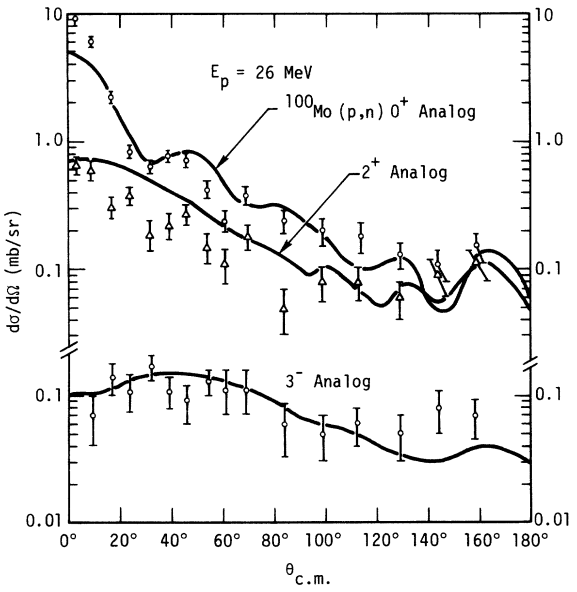

FIG. 8. Same as Fig. 6 but for ^{100}Mo.

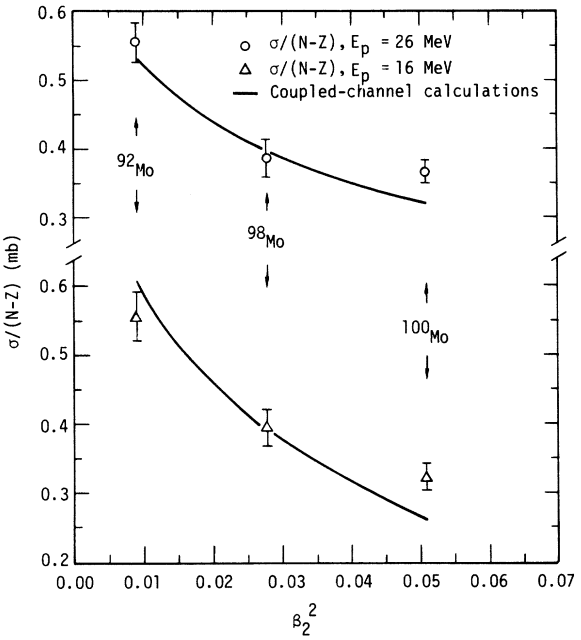

FIG. 9. Total reduced cross section $\sigma/(N-Z)$ as a function of β_2^2, showing the effect of a variation in the deformation parameter β_2 on the 0^+ analog cross section.

TABLE III. Mo(p,n) 2^+ analog cross sections in mb/sr at 18 MeV.

$\theta_{c.m.}$	^{98}Mo	^{100}Mo
3.5	0.58 ± 0.08	0.56 ± 0.08
9.2	0.35 ± 0.06	0.38 ± 0.06
17	0.36 ± 0.06	0.29 ± 0.06
24	0.34 ± 0.06	0.36 ± 0.07
32	0.48 ± 0.07	0.21 ± 0.06
39	0.29 ± 0.06	0.30 ± 0.06
46	0.18 ± 0.05	0.23 ± 0.05
54	0.18 ± 0.05	0.12 ± 0.035
61	0.18 ± 0.05	0.14 ± 0.04
69	0.08 ± 0.03	0.05 ± 0.025
84	0.14 ± 0.04	0.09 ± 0.03
99	0.13 ± 0.04	0.09 ± 0.03
114	0.06 ± 0.025	0.1 ± 0.03
129	0.21 ± 0.05	0.2 ± 0.055
144	0.07 ± 0.025	0.2 ± 0.06
159	0.03 ± 0.015	0.11 ± 0.04

TABLE IV. Mo(p,n) 2^+ and 3^- analog cross sections in mb/sr at 22 MeV.

	^{92}Mo		^{98}Mo		^{100}Mo	
$\theta_{c.m.}$	2^+	3^-	2^+	3^-	2^+	3^-
3.5	0.12 ± 0.03		0.42 ± 0.07		0.69 ± 0.075	0.1 ± 0.035
9.2	0.07 ± 0.02	0.065 ± 0.02	0.54 ± 0.08	0.06 ± 0.02	0.62 ± 0.07	0.12 ± 0.03
17	0.05 ± 0.015	0.057 ± 0.02	0.38 ± 0.08	0.04 ± 0.015	0.31 ± 0.045	0.11 ± 0.03
24	0.07 ± 0.015	0.09 ± 0.02	0.32 ± 0.08	0.05 ± 0.02	0.44 ± 0.06	0.11 ± 0.035
32	0.05 ± 0.01	0.11 ± 0.03	0.30 ± 0.07	0.07 ± 0.03	0.34 ± 0.05	0.08 ± 0.005
39	0.05 ± 0.01	0.10 ± 0.025	0.18 ± 0.05	0.05 ± 0.02	0.26 ± 0.05	0.13 ± 0.03
46	0.06 ± 0.015	0.076 ± 0.02	0.2 ± 0.05	0.06 ± 0.02	0.20 ± 0.04	0.16 ± 0.04
54	0.07 ± 0.015	0.11 ± 0.025	0.17 ± 0.05	0.1 ± 0.03	0.25 ± 0.04	0.14 ± 0.04
61	0.045 ± 0.01	0.07 ± 0.02	0.15 ± 0.04	0.12 ± 0.03	0.16 ± 0.03	0.10 ± 0.03
69	0.04 ± 0.01	0.053 ± 0.02	0.13 ± 0.04	0.08 ± 0.025	0.13 ± 0.03	0.13 ± 0.035
84	0.045 ± 0.01	0.068 ± 0.018	0.08 ± 0.025	0.11 ± 0.03	0.14 ± 0.03	0.12 ± 0.03
99	0.035 ± 0.01	0.068 ± 0.018	0.07 ± 0.025	0.06 ± 0.02	0.12 ± 0.03	0.11 ± 0.025
114	0.025 ± 0.01	0.046 ± 0.01	0.07 ± 0.025	0.08 ± 0.02	0.09 ± 0.025	0.07 ± 0.03
129	0.025 ± 0.01	0.068 ± 0.015	0.07 ± 0.025	0.05 ± 0.015	0.11 ± 0.03	0.06 ± 0.025
144	0.032 ± 0.01	0.034 ± 0.012	0.09 ± 0.03	0.04 ± 0.015	0.17 ± 0.04	0.12 ± 0.035
159	0.05 ± 0.01	0.065 ± 0.02	0.075 ± 0.025	0.045 ± 0.02	0.16 ± 0.04	0.06 ± 0.025

tudes using a coupled-channel code.[6]

The procedure for changing the BG global optical parameters for use in the coupled-channel calculation seems reasonable. The calculation of the dependence of the analog cross sections on $N-Z$ is obviously meaningless unless V_1 and W_1 are essentially uniform from isotope to isotope. We have also adopted the view that global optical parameters should apply after the coupling to strong states is taken into account explicitly. The coupling is less important to those states whose cross section is rather steady from isotope to isotope, since these effects should be accounted for by optical potentials. In our case the 2^+ inelastic cross section varies by a factor of about 5 from ^{92}Mo to ^{100}Mo, so it must be included explicitly. The cross section for the 3^- state varies much less, but enough that its inclusion should improve the calculations. When these six states are coupled together, it is expected that the global imaginary potentials of Ref. 9 must be reduced, and we adopted the rule that they must be reduced by the same percentage for all isotopes. It is likely that this procedure is still not rigorously correct, because there are transitions to other inelastic and rearrangement states[10] which will probably vary somewhat from isotope to isotope.

We have in this paper ignored the resonancelike structure in the energy dependence of the 0^+ analog cross section. The main effect of the resonance is in the neighborhood of 18–20 MeV. To avoid the effects of the resonance as much as possible we have used the data at 16 MeV to obtain the optical parameters and have fitted the $\sigma/(N-Z)$ dependence of the data at 26 MeV. It is, however, clear from the data that some resonance effects remain at 16 and 26 MeV. Although we are able to explain the $N-Z$ dependence of the cross section with the 2^+ and 3^- coupling at a given energy, we do not explain the energy dependence nor the variation of V_1 and W_1 from $1.2\times$ BG at 16 MeV to $0.9\times$ BG at 26 MeV. It is likely that some of this variation is a result of the resonance. Further, it is possible that some $N-Z$ dependence might result from differences in the energy dependence from isotope to isotope. A comparison of the energy dependence (Fig. 8 of Ref. 2) indicates that such an effect might in fact be the cause of the small disagreement between theory and experiment for ^{100}Mo in Fig. 9.

The resonance confuses the issue somewhat; however, the coupled-channel effects we have shown are on rather firm grounds, since the inelastic and analog couplings are empirical. The large variation in $\sigma/(N-Z)$, which is shown in the calculations, must be present in the charge-exchange reactions independent of the resonance. Furthermore, the variations of the analog cross section due to differences in energy dependence of the resonance from isotope to isotope are not great enough to mask the agreement between the coupled-channel calculations and the data.

TABLE V. Energy dependence of 2^+ analog cross sections.

E (MeV)	σ_{2^+} (mb) ^{98}Mo	^{100}Mo
18	1.99	1.80
22	1.55	2.08
26	.94	1.52

†Work performed under the auspices of the U.S. Energy Research and Development Administration.

*Summer visitor, 1974. Permanent address: Department of Physics, Oregon State University, Corvallis, Oregon 97331.

‡Permanent address: School of Physics and Astronomy, University of Minnesota, Minneapolis, Minnesota 55455.

[1]C. H. Poppe, S. M. Grimes, J. D. Anderson, J. C. Davis, W. H. Dunlop, and C. Wong, Phys. Rev. Lett. 33, 856 (1974).

[2]S. M. Grimes, C. H. Poppe, J. D. Anderson, J. C. Davis, W. H. Dunlop, and C. Wong, Phys. Rev. C 11, 158 (1975).

[3]V. A. Madsen, M. J. Stomp, V. R. Brown, J. D. Anderson, L. Hansen, C. Wong, and J. J. Wesolowski, Phys. Rev. Lett. 28, 629 (1972).

[4]Because in this case the one-step and two-step amplitudes are about 90° different in phase, the interference is also negligible.

[5]Coupling between the 2^+ and 3^- states is not expected to play an important role in the calculations and has therefore been neglected.

[6]M. J. Stomp, F. A. Schmittroth, and V. A. Madsen, USAEC Technical Report, Contract No. AT(45-1)-2227, Task Agreement No. 11 (unpublished).

[7]C. Wong, V. R. Brown, J. D. Anderson, J. C. Davis, S. M. Grimes, C. H. Poppe, and V. A. Madsen, Phys. Rev. C 11, 137 (1975).

[8]H. F. Lutz, D. W. Heikkinen, and W. Bartolini, Phys. Rev. C 4, 934 (1971).

[9]F. D. Becchetti and G. W. Greenlees, Phys. Rev. 182, 1190 (1969).

[10]L. D. Rickertson and P. D. Kunz, Phys. Lett. 47B, 11 (1973).